

The influence of chill thickness and austempering temperature on dry sliding wear behaviour of a Cu-Ni carbidic austempered ductile iron (CADI)

E. Akbarzadeh Chiniforush*, S. Yazdani**, V. Nadiran

Faculty of Materials Engineering, Sahand University of Technology, Tabriz, Iran

Received 28 February 2018, received in revised form 30 April 2018, accepted 6 June 2018

Abstract

The influence of chill thickness and applied load were studied on wear behaviour of a carbidic austempered ductile iron containing Cu and Ni. Ductile iron with chemical composition Fe-3.6C-2.6Si-0.53Cu-0.51Ni (in wt.%) was cast into standard moulds with copper end chills of different thicknesses. Wear test samples were prepared from the chilled surface of the blocks. Austenitizing heat treatment was carried out at 870 °C followed by austempering at 270, 320, 370 and 410 °C in electrically heated salt bath furnaces for optimum times. A block-on-ring testing machine was used to carry out wear tests in dry sliding condition under applied loads of 100 and 150 N. Scanning electron microscopy was used to examine the worn surface of the samples. The results indicated an improvement in wear resistance of austempered ductile iron by introducing carbides into the matrix compared to that of non-carbidic samples. Best wear performance in carbidic austempered ductile iron was achieved for a matrix containing about 30 vol.% carbides.

Key words: carbidic austempered ductile iron, sliding wear, chill thickness, block-on-ring

1. Introduction

Austempered Ductile Iron (ADI) has long been recognized for its combination of high strength and toughness replacing forged steel components in many applications. It is also well known that this alloy performs very well under different wear mechanisms such as rolling contact fatigue, adhesion and abrasion [1–8]. ADI has proved to behave properly under different conditions, and it is possible to obtain good performance in wear if the heat treatment parameters are selected properly [9–14]. The austempering reaction in ductile irons is a two-stage process that differs considerably from the single-stage bainite reaction in steels [15]. In steel, it is a single step process in which austenite transforms directly to bainite [16] whereas in ductile iron it is a two-step process. In the first step, austenite (γ) transforms to acicular ferrite (α) (or ferrite and carbide) and high carbon austenite (γ_H). In the second step, when the casting is austempered longer than required, the matrix de-

composes to form more stable ferrite and carbide [12]. Austempering temperature is the primary heat treatment variable which directly affects the final mechanical properties. Strength and hardness are influenced by the austempering temperature chosen. By increasing the austempering temperature, the volume fraction of austenite and the thickness of ferrite layers at the end of stage I reaction increase, meanwhile the amount of carbides decreases at this time [17].

A new type of ADI which contains carbides immersed in the typical matrix of ductile iron called carbidic austempered ductile iron (CADI) has been developed in recent years. CADI is produced by austempering heat treatment of ductile iron which has a controlled amount of carbides present in the microstructure for a higher abrasion resistance than that of the base material [18–20]. The standard practice in carbide introduction is chill-cast of ductile iron parts. Depending on the chill thickness and type the desired amount of carbides can be introduced to the surface of the casting. The typical range of carbides which are

*Corresponding author: e-mail address: e-akbarzadeh@sut.ac.ir

**Corresponding author: e-mail address: yazdani@sut.ac.ir

present in the microstructure is within 10–30 vol.% [21, 22]. The resulting microstructure consists of carbides in the ausferrite matrix. CADI is more wear resistant than Grade 1600 (GR 5) ADI, less expensive and tougher than many abrasion resistant irons and can replace Mn steels at an equal or lower cost [23]. The carbides improve the abrasion wear resistance. If the heat treatment parameters and chemical composition of the alloy are controlled properly, the maximum abrasion resistance can be achieved. To obtain as-cast carbides, it is essential to reduce the amount of graphitizing elements, e.g., Si, in order to promote the precipitation of carbides during eutectic solidification of ductile iron [21, 25]. The other option is to add the carbide stabilizing elements into the melt, such as chromium, molybdenum or titanium. They strongly reduce the stable and metastable interval between eutectic temperatures and promote the solidification according to the metastable diagram. The under-cooling also affects the size and number of solidification eutectic cells and subsequently the microsegregation. By lowering the cooling rate, the microsegregation increases. This results in the probability of the formation of carbides at the last into freeze areas [26]. The cooling rate and chemical composition of alloy affect the size and composition of carbides which may vary from ledeburitic to thin plate-shaped carbides. Ledeburitic carbides which are formed by controlling the cooling rate or reducing silicon content in unalloyed ductile irons are less stable than alloyed ones and have higher tendency to dissolve during the austenitizing process [27, 28].

The main objective of this work is to study the effect of chill thickness on the formation of carbides on a ductile cast iron surface to obtain the so-called carbidic austempered ductile iron and then to evaluate the sliding wear behaviour of the alloy at different austempering heat treatment conditions.

2. Experimental procedure

2.1. Alloy and heat treatment process

The ductile iron was melted in a rotary furnace then cast into the sand mould according to AFS standard as illustrated in Fig. 1 [29]. Three different copper chill thicknesses were used to obtain different amount and depths of carbides in the chilled layer. The chemical composition of iron is given in Table 1.

Wear test samples were cut and prepared from the chilled section with the dimension of 10 mm × 10 mm × 20 mm. The heat treatment was carried out using an electrically heated salt bath furnace at 870 °C for 90 min followed by subsequent rapid cooling to the austempering salt bath furnaces operating in the temperature range of 270–410 °C for 4 h.

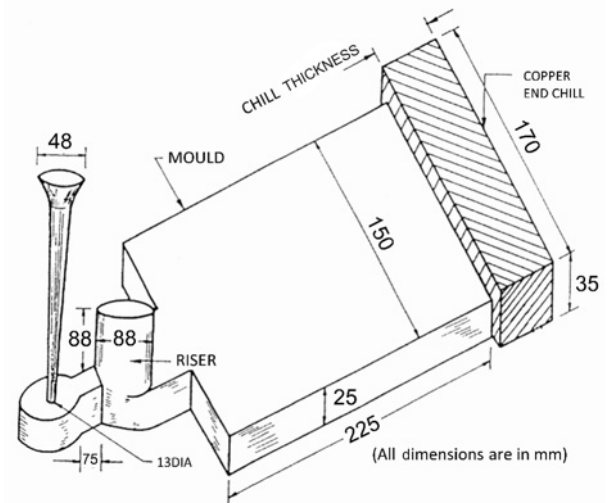


Fig. 1. Experimental setup (AFS standard mould showing copper end chill block location).

Table 1. The composition of ductile iron (wt.%)

Mn	Ni	Cu	P	S	Si	C
0.2	0.5	0.53	0.014	0.013	2.6	3.6

2.2. Microstructural evaluations

Samples for metallographic examination were ground and polished following the standard procedures after heat treatment. 2% Nital etching solution and subsequent etching in sodium metabisulfite 20% solution were used to reveal the microstructure. Microstructural evaluations were conducted on Olympus PMG3™ optical microscope and Cam Scan MV-2300™ scanning electron microscope (SEM) operating at 30 kV. The samples carbide volume fraction was measured according to ASTM E562-11 [30] standard test method on polished and etched samples. Image analysis was used to determine the nodule count according to ASTM E2567-16a [31] standard test method.

2.3. Wear tests

Dry sliding wear tests were performed on samples according to ASTM G77-98 standard using a block-on-ring wear test machine specially built for laboratory use on samples. The wear test for all samples was conducted under the normal loads of 100 and 150 N and a sliding velocity of 3.7 m s⁻¹. The samples weight loss was then measured at 10 min intervals for a total test time of 40 min. The worn surface of samples was also studied using the Cam Scan MV-2300™ SEM to determine the wear mechanism.

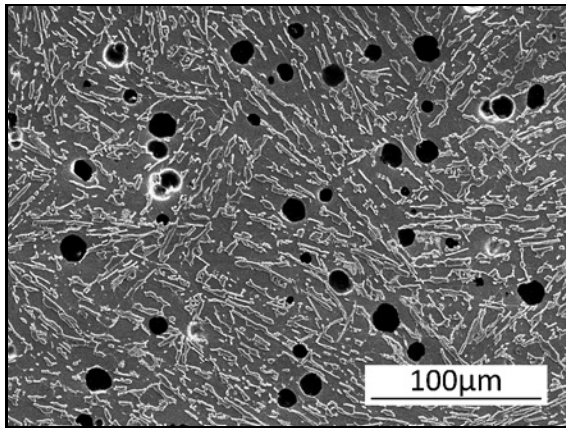


Fig. 2. The SEM micrograph of the chilled surface consisting of ledeburite (carbide and transformed austenite to martensite/bainite).

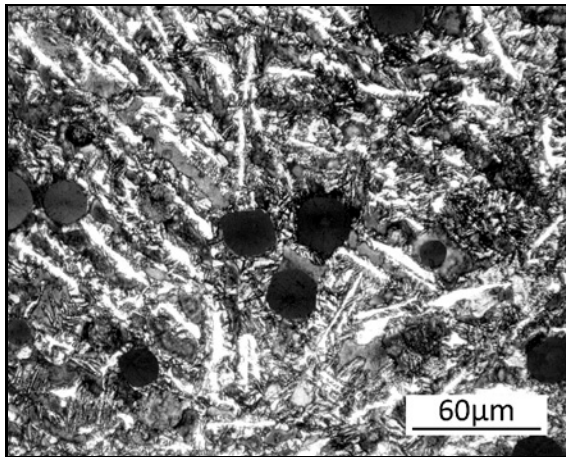


Fig. 3. Typical microstructure of sample austempered at 370 °C for 240 min near the chilled surface, consisting of iron carbides and graphite nodules within the ausferritic matrix.

2.4. Hardness measurements

Rockwell C hardness scale was used to measure the hardness. A total number of six hardness measurements at different locations were taken. The average values were calculated and used for the analysis. The cross section hardness was measured for all samples using a microhardness tester with an applied load of 50 gr.

3. Results and discussion

3.1. The microstructure of chilled and austempered samples

The SEM micrograph from the chilled surface is

Table 2. The nodule counts and carbide vol.% of samples with different chill thicknesses

Chill thickness (mm)	Nodule count (mm^{-2})	Carbide volume (%)
35	300	45
25	250	39
15	190	30

shown in Fig. 2. The microstructure consists of ledeburite (carbides and transformed austenite to martensite/bainite). The nodule count is about 300 mm^{-2} for the copper chill of 35 mm thickness.

Away from the chilled surface, the nodule count decreases gradually and reaches to about 100 mm^{-2} where there is not much effect on the cooling rate by the block. The chill thickness influences the nodule count as well as the carbide volume. In Table 2 the nodule counts and the carbide volume are presented for different chill thicknesses. Thicker blocks caused higher cooling rates during solidification, and consequently higher nodule counts and carbide volume acquired.

Figure 3 shows typical microstructure of austempered samples near the chilled surface after austempering at 370 °C. The microstructure of CADI consists of iron carbides and graphite nodules within the ausferritic matrix. The matrix is much harder compared to graphite nodules. The type of carbide morphology and distribution which was observed near the chilled surface results in a wear resistant and tough material. Figure 4 shows the microstructural changes observed during austempering in the present study away from the chill block and shows the features as described. Figure 4a shows how acicular ferrite has started to form in regions surrounding the graphite nodules after austempering for 2 min at 370 °C. The remaining matrix areas show martensite which has been formed from the low carbon unreacted austenite during cooling to room temperature from the austempering temperature. Figure 4b shows that the ausferrite reaction is almost completed in the eutectic cell and intercellular boundary regions after 60 min. The platelet structure of the ausferrite is evident in the microstructure. Figure 4c shows that the platelet structure is no longer clearly defined after 1140 min owing to the onset of the stage II reaction.

3.2. The effect of chill thickness and austempering temperature on hardness

The variations of hardness vs. distance from the chilled surface to the core are shown in Fig. 5 for the chill thicknesses studied. Hardness is higher at similar points for thicker chilled samples which produces

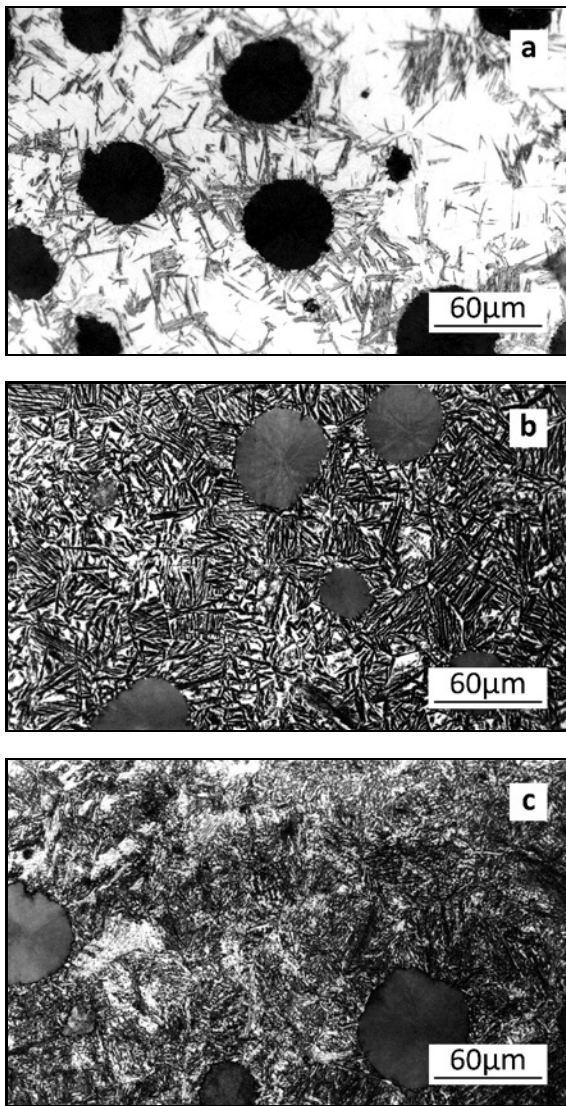


Fig. 4. Microstructures of samples austempered at 375 °C for (a) 2 min, (b) 60 min and (c) 1140 min (optical).

higher cooling rates and more carbide in the matrix. Away from the surface, hardness decreases with decreasing carbide volume.

The variation of hardness with austempering temperatures of different chill thickness samples is shown in Fig. 6. It is seen that hardness decreases with increasing the austempering temperature from 270 to 370 °C, then it increases as the austempering temperature further increases to 410 °C. The initial decrease is a consequence of coarse ausferritic microstructure. Austempering temperature has a direct influence on the strength and hardness of the matrix in ADI [32, 33]. The next increase in hardness is because of the increased volume of blocky austenite the central region of which transformed to martensite during cooling to room temperature. This behaviour in ADI is reported elsewhere [4, 5].

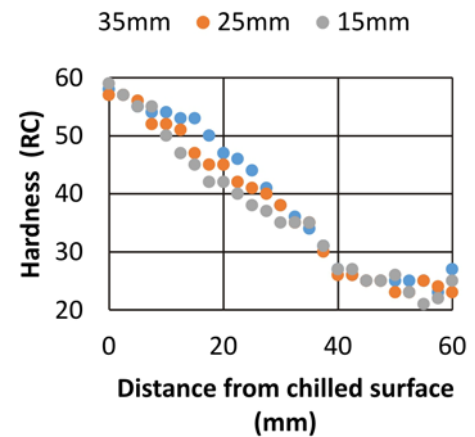


Fig. 5. The change in hardness with distance from the chill surface for various chill thicknesses.

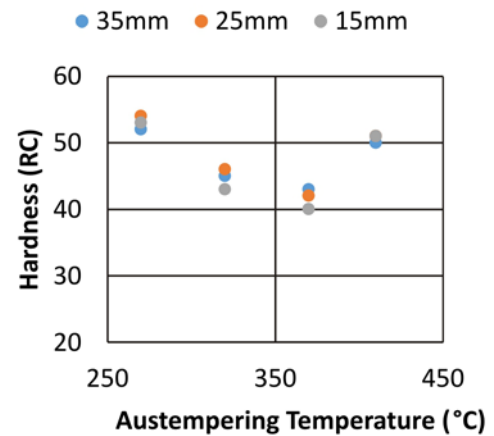


Fig. 6. The variation of hardness with austempering temperature for various chill thicknesses.

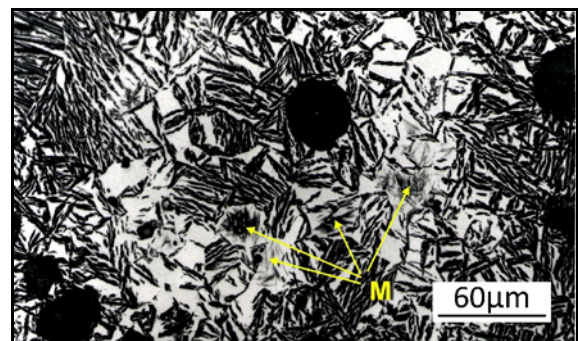


Fig. 7. The microstructure of a sample austempered at 410 °C. The arrows show the transformed region of blocky austenite to martensite.

The transformed regions of blocky austenite to martensite are shown by arrows in Fig. 7 for a sample austempered at 410 °C.

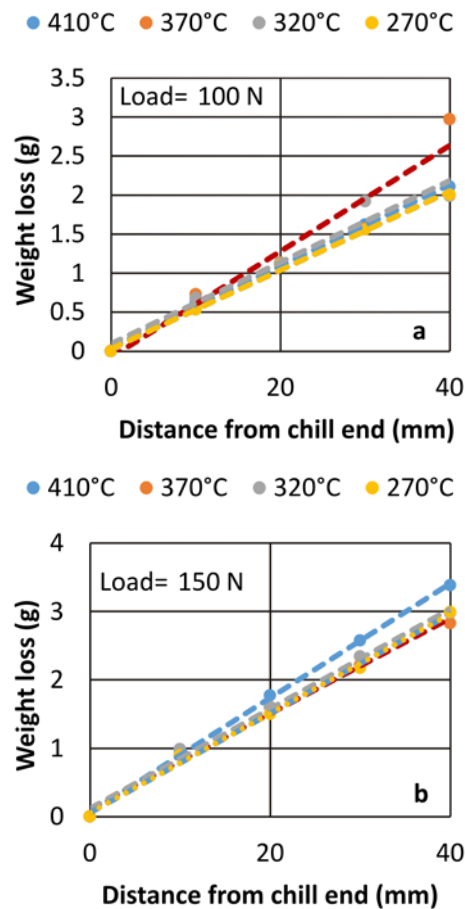


Fig. 8. The variations of weight loss with test time for applied loads of 100 and 150 N. Chill thickness is 35 mm and the austempering temperature is 410°C.

3.3. Effect of austempering temperature on wear behaviour

The variations in weight loss with time for applied loads of 100 and 150 N and chill thickness of 35 mm at the austempering temperature of 410°C are shown in Fig. 8. It is evident that wear behaviour is affected by the applied load. The effect of increasing the applied load is to increase the weight loss at a given distance travelled. Several factors can influence the wear behaviour of CADI in the current study, for instance, ausferrite morphology, carbide vol.% and also graphite nodules fraction in the matrix. Ausferrite morphology is influenced directly by austempering heat treatment whereas the carbides and graphites volume and morphology are determined by the cooling rate, i.e., chill thickness. Figure 8 displays that the wear resistance of CADI is not influenced by austempering temperature significantly and it is slightly higher for the austempering temperature of 410°C. The matrix at the highest austempering temperature of 410°C involves coarser ausferrite and more regions of blocky austenite. It ap-

pears that the transformation of these less mechanically stable austenites improved the wear resistance of CADI moderately. The higher the austempering temperature the higher the toughness [12]. The combination of toughness and hardness at this temperature can explain the better wear performance of CADI. This implies that the matrix toughness is as important as hardness in wear behaviour of CADI.

3.4. Effect of chill thickness on the wear behaviour

The results indicate that thick chilled samples have a higher carbide and lower graphite volumes compared to the thin chilled samples. The graphites are also finer in these samples. The morphology and the carbide and graphite volume all influence the wear resistance of CADI. The beneficial effect of graphites on wear resistance of austempered ductile irons has been reported previously [34]. Hatate et al. [35] proposed that changing graphite shape from spheroidal to flake was found to result in a considerable increase in weight loss of ADI both in dry and wet conditions. In another research Sugishita et al. [36] indicated that formation of graphite layers on the wear surface of cast iron contributes to the protection of metallic contact points. Carbides have a beneficial influence on enhancing wear resistance when they are large enough in relation to the size of the abrasive. Albertine et al. [37] have shown that in white cast irons, increasing the carbide volume from 13 to 41 % resulted in a decrease in wear rates. Sapate et al. [38] reported that the variation in erosion rate with carbide volume fraction was observed to be a strong function of the erodent particle hardness, impingement angle and the impact velocity.

The effect of chill thickness on the variation of weight loss is shown in Fig. 9 for the austempering temperature of 270, 320, 370 and 410°C at applied loads of 100 and 150 N. It was anticipated that the thick chilled samples would display a better wear performance. However, the results do not appear to support this and the 35 and 25 mm thick chilled samples show more weight loss. It seems that even though the carbide vol.% is higher for 35 and 25 mm thick chilled samples, a lower graphite content as a lubricant had a stronger contribution to the wear performance of CADI. At a higher applied load of 150 N, the contribution of graphite as lubricant decreases. This confirms the previous findings of Sugishita and Fujiyoshi [39]. Several researchers have also stated the role of graphite as a lubricant at low applied loads [23, 40, 41]. Research carried out by Zum Gahr and El-dis [42] supports our findings as their results indicate that approximately 28 vol.% carbide provides the best abrasion resistance for white cast irons. In the current study, the samples of 15 mm thick chills consisted of about 30 vol.% carbide.

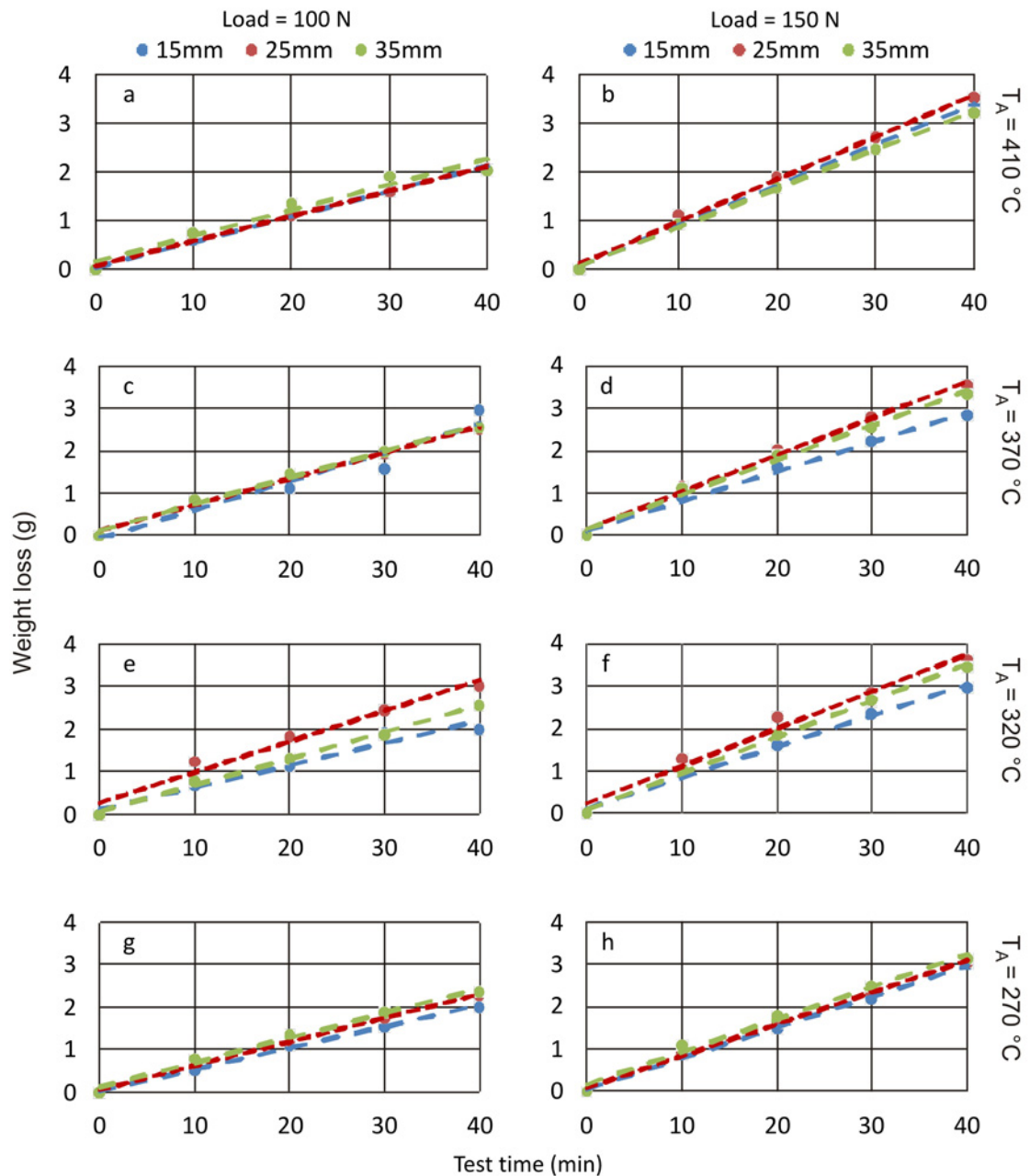


Fig. 9a–h. The variation of weight loss with test time for various chill thicknesses and austempering temperatures at applied loads of 100 and 150 N.

Abrasive wear is classified based on the contact type and environment [43]. Two modes are known as two-body and three-body abrasive wear. The two-body mode of wear occurs when the hard particles detach the material from the opposite surface. In fact, the material is removed or displaced by a cutting or plowing operation. The three-body wear happens when the particles are free to move and slide on a surface. At the higher load of 150 N, the adhesion between surfaces followed by tearing of the material below the surface has caused the galling of material. This is evident in Figs. 10a,b. The wear particles are detached

by the cyclic crack growth of microcracks on the surface. The microcracks are either superficial cracks or subsurface cracks. The microcracks are indicated in Fig. 9b with arrows. The scratches on the wear surfaces are deepened with time. Fragmentation occurs when the material is separated from the worn surface by a cutting process and the indenting abrasive causes localized fracture of the wear material. These cracks then freely propagate locally around the wear groove, resulting in additional material removal by spalling [43]. Oxide debris is created during the sliding motion of surfaces. It is originated from interactions among

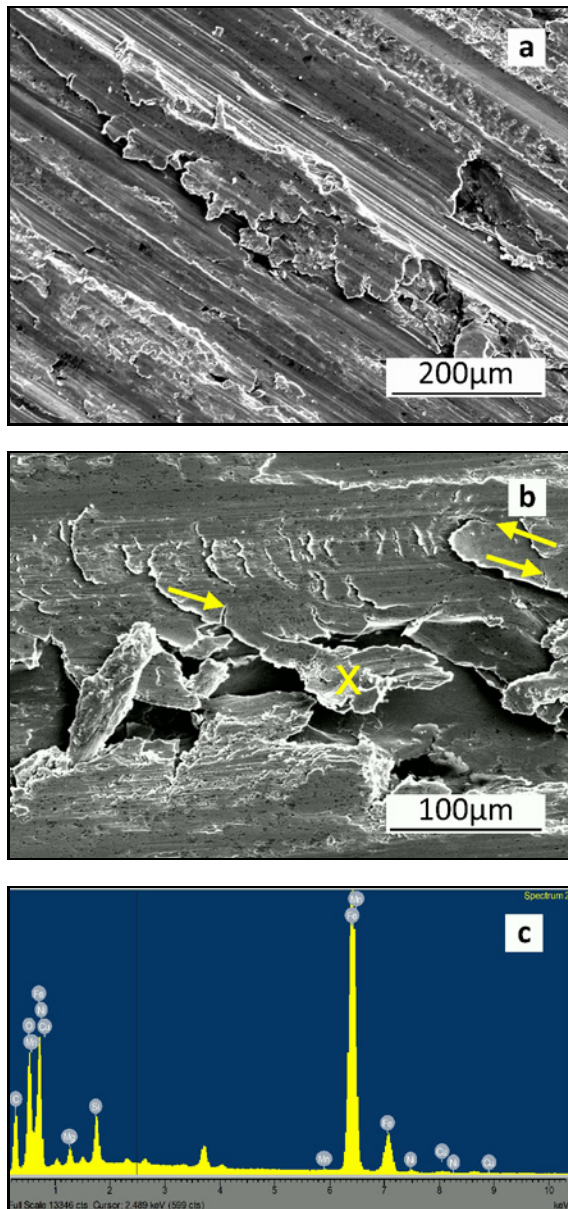


Fig. 10. SEM micrograph of worn surface indicating: (a) galling of the material, (b) micro-cracks, and (c) EDS microanalysis of the indicated detaching particle (X) in (b).

the worn surfaces and environmental causes, i.e., humidity. The EDS microanalysis of the detaching area in Fig. 10b (indicated as X) is shown in Fig. 10c that reveals the particle is iron oxide. According to the results, the main wear mechanism is three-body abrasive wear. In previous work, it was shown that graphite nodules near the surface could act as cracks beneath the surface [9]. As a result, cracks nucleation happens with no difficulty and consequently cracks propagation controls the wear in ductile irons [44].

Comparing the results of this study and a previous study on ADI [9] at similar testing conditions shows that CADI is more wear resistant than ADI with sim-

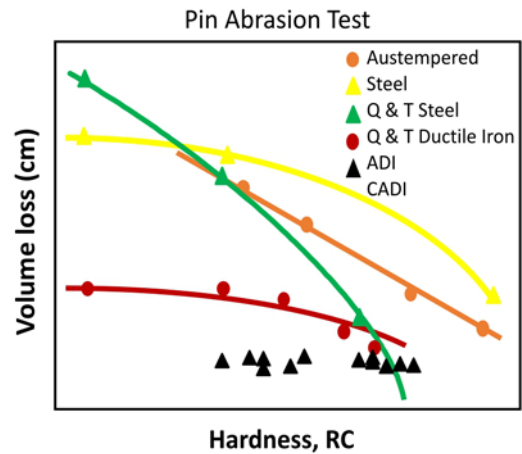


Fig. 11. Pin abrasion test chart for austempered steel, Q&T steel, Q&T ductile iron, ADI [49] and CADI.

ilar heat treatment conditions. This is the direct result of the presence of continuous carbides network within the matrix. The wear resistance is related to the mechanical properties of the material, i.e., hardness and toughness. The most important parameter is hardness which has a strong effect on the wear behaviour. This effect can be divided into the effects of bulk and microconstituents' hardness, i.e., microhardness. The microstructure has a considerable influence on the mechanical properties and wear resistance [45]. Carbides are important in the microstructures since they influence the wear behaviour strongly because they are normally much harder than the matrix. The volume fraction of carbides is a relatively useful parameter in alloys, and in most cases, wear resistance increases with an increase of carbide volume fraction [46]. It has been reported that in steels the wear resistance increases directly with the volume of the hard constituent, i.e., carbides, particularly with massed carbides [47]. The carbides present in within the microstructure of CADI have continuous nature as indicated in SEM micrograph in Fig. 2. When carbides distribute in the form of separate isles they can be detached from the matrix easily and may have less influence on wear resistance [48]. In the case of CADI, the continuous and massive nature of carbides has improved the wear resistance considerably as compared to wear test results for ADI [9].

3.5. Comparing wear behaviour with other alloys

Figure 11 shows the pin abrasion test graph for austempered steel, quenched and tempered steel, ductile iron, ADI [49] and CADI normalised results with previous work on ADI [50]. In previous works [9, 50] it was demonstrated that the weight loss was over 4 g for

ADI specimens at the same test conditions. In present work, CADI of same base composition has shown a better performance when the weight loss is within the range of 3–3.5 g.

4. Conclusions

Studying the influence of chill thickness and austempering temperature on wear behaviour of a carbide austempered ductile iron with composition of Fe-3.6C-2.6Si-0.53Cu-0.51Ni (in wt.%) the following conclusions can be drawn:

– Copper chill thickness influences the nodule count, carbides and graphite volume. For 35, 25 and 15 mm chill blocks the nodule counts were about 300, 250 and 190 mm⁻², respectively. By increasing the chill thickness, the carbide volume increases within the range 30–45 % and graphite volume decreases.

– Best wear performance achieved for a matrix containing about 30 vol.% carbide. Increasing the carbide volume by using thicker chills does not enhance the wear performance of CADI. This behaviour is related to higher vol.% of graphite as a lubricant which contributes more to wear performance at thinner chills.

– Hardness is higher at same distances from the chilled surface to the core of thicker chilled samples as a result of more carbide in the matrix. Far from the chilled face, hardness decreases for all samples as carbide content decreases.

– Abrasive wear was the main wear controlling mechanism in CADI.

– EDS microanalyses of a delaminated wear debris showed the formation of iron oxide during wear test. Scratches and scars on the wear surface are thought to be caused by this oxide debris that retains between the rubbing surfaces.

– According to results of this study and previous findings [9] it can be concluded that CADI is more wear resistant than quenched and tempered steel and ductile iron at the same level of hardness.

Acknowledgement

Authors are grateful to the Sahand University of Technology for providing the research facilities and financial support.

References

- [1] Rajnovic, D., Eric, O., Sidjanin, L.: *Kovove Mater.*, 50, 2012, p. 199. [doi:10.4149/km_2012_3_199](https://doi.org/10.4149/km_2012_3_199)
- [2] Benam, A. S., Yazdani, S., Avishan, B.: *China Foundry*, 8, 2011, p. 325.
- [3] Ardestani, M., Yazdani, S.: *China Foundry*, 4, 2007, p. 120.
- [4] Yazdani, S., Elliott, R.: *Materials Science and Technology*, 15, 1999, p. 531. [doi:10.1179/026708399101506247](https://doi.org/10.1179/026708399101506247)
- [5] Yazdani, S., Elliott, R.: *Materials Science and Technology*, 15, 1999, p. 541. [doi:10.1179/026708399101506076](https://doi.org/10.1179/026708399101506076)
- [6] Yazdani, S., Elliott, R.: *Materials Science and Technology*, 15, 1999, p. 896. [doi:10.1179/026708399101506698](https://doi.org/10.1179/026708399101506698)
- [7] Yazdani, S., Elliott, R.: *Materials Science and Technology*, 15, 1999, p. 885. [doi:10.1179/026708399101506698](https://doi.org/10.1179/026708399101506698)
- [8] Dorazil, E.: *High Strength Austempered Ductile Cast Iron*. Amsterdam, Ellis Horwood 1991.
- [9] Akbarzadeh Chiniforush, E., Rahimi, M. A., Yazdani, S.: *China Foundry*, 13, 2016, p. 361. [doi:10.1007/s41230-016-6072-0](https://doi.org/10.1007/s41230-016-6072-0)
- [10] Likhite, A., Parhad, P., Peshwe, D., Pathak, S.: *World Academy of Science, Engineering and Technology, International Journal of Chemical, Molecular, Nuclear, Materials and Metallurgical Engineering*, 8, 2014, p. 510. <http://scholar.waset.org/1307-6892/9998458>
- [11] Katuku, K., Koursaris, A., Sigalas, I.: *Wear*, 268, 2010, p. 294. [doi:10.1016/j.wear.2009.08.027](https://doi.org/10.1016/j.wear.2009.08.027)
- [12] Avishan, B., Yazdani, S., Jalali Vahid, D.: *International Journal of Cast Metals Research*, 24, 2011, p. 22. [doi:10.1179/136404610X12816241546654](https://doi.org/10.1179/136404610X12816241546654)
- [13] Avishan, B., Yazdani, S., Jalali Vahid, D.: *Materials Science and Engineering A*, 523, 2009, p. 93. [doi:10.1016/j.msea.2009.05.044](https://doi.org/10.1016/j.msea.2009.05.044)
- [14] Harding, R.: *Kovove Mater.*, 45, 2007, p. 1.
- [15] Avishan, B., Garcia-Mateo, C., Yazdani, S., Caballero, F. G.: *Materials Characterization*, 81, 2013, p. 105. [doi:10.1016/j.matchar.2013.04.015](https://doi.org/10.1016/j.matchar.2013.04.015)
- [16] Miab, S. A., Avishan, B., Yazdani, S.: *Acta Metallurgica Sinica (English Letters)*, 29, 2016, p. 587. <http://link.springer.com/journal/40195>
- [17] Voigt, R.: *Cast Met.*, 2, 1989, p. 71. [doi:10.1080/09534962.1989.11818986](https://doi.org/10.1080/09534962.1989.11818986)
- [18] Lagarde, M., Basso, A., Dommarco, R. C., Sikora, J.: *ISIJ International*, 51, 2011, p. 645. [doi:10.2355/isijinternational.51.645](https://doi.org/10.2355/isijinternational.51.645)
- [19] Sebastián, L., Sikora, J. A., Dommarco, R. C.: *Key Engineering Materials*, 457, 2011, p. 187. [doi:10.4028/www.scientific.net/KEM.457.187](https://doi.org/10.4028/www.scientific.net/KEM.457.187)
- [20] Keough, J., Hayrynen, K.: *Ductile Iron News*, 3, 2000, p. 123.
- [21] Laino, S., Sikora, J., Dommarco, R. C.: *ISIJ International*, 50, 2010, p. 418. [doi:10.2355/isijinternational.50.418](https://doi.org/10.2355/isijinternational.50.418)
- [22] Hemanth, J.: *Materials & Design*, 21, 2000, p. 139. [doi:10.1016/S0261-3069\(99\)00101-6](https://doi.org/10.1016/S0261-3069(99)00101-6)
- [23] Hayrynen, K., Brandenburg, K.: *AFS Transactions*, 111, 2003, p. 845.
- [24] Patil, S., Likhite, A., Pathak, S.: *Indian Foundry Journal*, 58, 2012, p. 9652.
- [25] Laino, S., Sikora, J., Dommarco, R.: *Wear*, 265, 2008, p. 1. [doi:10.1016/j.wear.2007.08.013](https://doi.org/10.1016/j.wear.2007.08.013)
- [26] Akbarzadeh Chiniforush, E., Iranipour, N., Yazdani, S.: *China Foundry*, 13, 2016, p. 217. [doi:10.1007/s41230-016-6034-6](https://doi.org/10.1007/s41230-016-6034-6)

- [27] Peng, Y.-C., Jin, H.-J., Liu, J.-H., Li, G.-L.: *Materials Characterization*, 72, 2012, p. 53. [doi:10.1016/j.matchar.2012.07.006](https://doi.org/10.1016/j.matchar.2012.07.006)
- [28] Laino, S., Sikora, J. A., Dommarco, R. C.: *ISIJ International*, 49, 2009, p. 1239. [doi:10.2355/isijinternational.49.1239](https://doi.org/10.2355/isijinternational.49.1239)
- [29] Yogeska, K. B., Hemanth, J.: *International Journal of Advanced Engineering Research and Studies*, 1, 2012, p. 240.
- [30] ASTM E562-11. Standard Test Method for Determining Volume Fraction by Systematic Manual Point Count. West Conshohocken, ASTM International 2011. [doi:10.1520/E0562-11](https://doi.org/10.1520/E0562-11)
- [31] ASTM E2567-16a. Standard Test Method for Determining Nodularity And Nodule Count In Ductile Iron Using Image Analysis. West Conshohocken, ASTM International 2016. [doi:10.1520/E2567-16A](https://doi.org/10.1520/E2567-16A)
- [32] Yazdani, S., Bayati, H., Elliott, R.: *International Journal of Cast Metals Research*, 13, 2001, p. 317. [doi:10.1080/13640461.2001.11819413](https://doi.org/10.1080/13640461.2001.11819413)
- [33] Yazdani, S., Elliott, R.: *Mo Alloyed Austempered Ductile Irons*. Indianapolis, Minerals, Metals & Materials Society 1996.
- [34] Ghaderi, A., Ahmadabadi, M. N., Ghasemi, H.: *Wear*, 255, 2003, p. 410. [doi:10.1016/S0043-1648\(03\)00156-X](https://doi.org/10.1016/S0043-1648(03)00156-X)
- [35] Hatate, M., Shiota, T., Takahashi, N., Shimizu, K.: *Wear*, 251, 2001, p. 885. [doi:10.1016/S0043-1648\(01\)00746-3](https://doi.org/10.1016/S0043-1648(01)00746-3)
- [36] Sugishita, J., Fujiyoshi, S.: *Wear*, 66, 1981, p. 209. [doi:10.1016/0043-1648\(81\)90115-0](https://doi.org/10.1016/0043-1648(81)90115-0)
- [37] Albertin, E., Sinatora, A.: *Wear*, 250, 2001, p. 492. [doi:10.1016/S0043-1648\(01\)00664-0](https://doi.org/10.1016/S0043-1648(01)00664-0)
- [38] Sapate, S., Rao, A. R.: *Wear*, 256, 2004, p. 774. [doi:10.1016/S0043-1648\(03\)00527-1](https://doi.org/10.1016/S0043-1648(03)00527-1)
- [39] Sugishita, J., Fujiyoshi, S.: *Wear*, 68, 1981, p. 7. [doi:10.1016/0043-1648\(81\)90015-6](https://doi.org/10.1016/0043-1648(81)90015-6)
- [40] Owjadi, A., Hedjazi, J., Davami, P.: *Materials Science and Technology*, 14, 1998, p. 245. [doi:10.1179/mst.1998.14.3.245](https://doi.org/10.1179/mst.1998.14.3.245)
- [41] Landsdown, A., Price, A.: *Materials Engineering Practice Series*. Oxford, Pergamon Press 1986.
- [42] Zum Gahr, K.-H., Eldis, G. T.: *Wear*, 64, 1980, p. 175. [doi:10.1016/0043-1648\(80\)90101-5](https://doi.org/10.1016/0043-1648(80)90101-5)
- [43] George E. Totten (ed.): *ASM Handbook: Friction, Lubrication, and Wear Technology*. Volume 18. Materials Park, ASM International 1992.
- [44] Perez, M., Cisneros, M., Lopez, H.: *Wear*, 260, 2006, p. 879. [doi:10.1016/j.wear.2005.04.001](https://doi.org/10.1016/j.wear.2005.04.001)
- [45] Moore, M.: *Wear*, 27, 1974, p. 1. [doi:10.1016/0043-1648\(74\)90080-5](https://doi.org/10.1016/0043-1648(74)90080-5)
- [46] Zum Gahr, K.-H.: *Microstructure and Wear of Materials*. London, Elsevier Science 1987.
- [47] Silence, W. L.: *ASME J. Lubr. Technol.*, 100, 1978, p. 428. [doi:10.1115/1.3453203](https://doi.org/10.1115/1.3453203)
- [48] Zum Gahr, K.-H.: *Tribology International*, 31, 1998, p. 587. [doi:10.1016/S0301-679X\(98\)00079-6](https://doi.org/10.1016/S0301-679X(98)00079-6)
- [49] Hayrynen, K. L.: *Modern Casting*, 85, 1995, p. 35.
- [50] Yazdani, S., Rahimi, M.: *Materials Science Forum*, 475–479, 2005, p. 199. [doi:10.4028/www.scientific.net/MSF.475-479.199](https://doi.org/10.4028/www.scientific.net/MSF.475-479.199)